

D. ROMANINI<sup>1,✉</sup>  
M. CHENEVIER<sup>1</sup>  
S. KASSI<sup>1</sup>  
M. SCHMIDT<sup>2</sup>  
C. VALANT<sup>2</sup>  
M. RAMONET<sup>2</sup>  
J. LOPEZ<sup>3</sup>  
H.-J. JOST<sup>3</sup>

# Optical–feedback cavity–enhanced absorption: a compact spectrometer for real–time measurement of atmospheric methane

<sup>1</sup> Laboratoire de Spectrométrie Physique CNRS UMR5588, Université J. Fourier–Grenoble, Saint Martin d’Hères, France  
<sup>2</sup> Laboratoire des Sciences du Climat et de l’Environnement UMR CEA-CNRS 1572, 91198 Gif-sur-Yvette, France  
<sup>3</sup> Bay Area Environmental Research Institute, 560 Third St. West, Sonoma, CA 95476, USA

Received: 7 November 2005/  
Revised version: 23 February 2006  
Published online: 22 April 2006 • © Springer-Verlag 2006

**ABSTRACT** We report on the application of the new technique of optical–feedback cavity–enhanced absorption spectroscopy to the real–time quantitative measurement of tropospheric methane traces from an airplane using a compact, low cost instrument based on a telecommunication–type diode laser operating close to room temperature. Methane concentration is obtained by fitting the absorption line centered at 1658.96 nm ( $6026.23\text{ cm}^{-1}$ ) which belongs to the first overtone transition of the CH stretch vibration. The measurement rate is about 30 Hz, but the response time is limited to about 0.3 s by the gas flow in the measurement cell. The instrument provides the absolute ambient methane concentration accurate to  $\pm 1\%$  ( $\pm 20$  ppb) without need for a periodic calibration. This is demonstrated by a hands–off comparison with a self–calibrating chromatographic setup during 10 days. The observed measurement stability can be extrapolated to much longer time periods. With respect to the short–term performance (minutes) fast concentration changes at the level of 1 ppb can be detected, and we believe this performance can be extended to the long term. Finally, a laboratory comparison with a lead–salt mid–infrared diode laser multipass spectrometer (operating close to  $3028\text{ cm}^{-1}$  at liquid nitrogen temperature) demonstrates a similar performance.

PACS 07.88.+y; 42.55.Px; 42.62.Fi

## 1 Introduction

Methane is the second most important greenhouse gas with both anthropogenic (e.g. agriculture, natural gas) and natural emissions (e.g. wetlands). Sources and sinks are still not well understood and hence the large variability in the rate of increase over the last decade is poorly explained by models [1–3]. Methane is also related to the third most important greenhouse gas, ozone, through its reaction with OH, which further complicates the prediction of future levels of methane [1, 4, 5].

The recent paper by Bergamaschi et al. [6] has demonstrated that quasi–continuous observations close to source

regions provide significant constraints on the regional distribution of the emissions. However, the limited number of high precision in situ measurement sites (about 20 distributed in the world) is largely insufficient to establish an operational emission monitoring system. In addition, the cost and complexity of the currently used gas chromatographs limits their broad deployment in a global monitoring network. Small, field deployable instruments are needed to better quantify strength of sources and sinks and to improve forecasts of methane concentrations.

Accurate measurements of methane and other trace gases in the free troposphere aboard aircraft enable identification of the source regions of air masses. High precision measurements of the CH<sub>4</sub> vertical profiles will be valuable in the future network to validate the parameterisation of vertical transport in atmospheric models, and also to validate remote sensing measurements from the ground [7] or satellite platforms [8] which are currently being deployed.

Laser spectroscopy is recognized for its ability to provide fast and selective measurement of trace concentrations in the gas phase. In particular, optical absorption methods have the advantage of enabling the determination of the concentration of a molecule directly from the intensity of one of its absorption lines. The conditions of absorption measurements are easily controlled to guarantee a highly linear, reproducible, quantitative response. To achieve sufficient sensitivity usually the strongest absorption lines in the mid infrared and belonging to a fundamental vibrational transition are accessed. This can be done by using either a lead–salt diode laser (LSD), a quantum cascade laser (QCL), difference frequency generation (DFG), or an optical parametric oscillator laser (OPO). While LSDs need low power to operate, they work at liquid nitrogen temperatures and their optical power is only a few hundreds  $\mu\text{W}$ . QCLs yield high optical power, but are often not readily available at the desired wavelength, mostly operate at room temperature only in pulsed mode, and are tunable over a small spectral range [9, 10]. DFG sources are rather bulky and produce low power levels (mW at best) [11]. OPOs are mechanically complex and fragile and difficult to tune continuously over wide spectral ranges [12]. In addition, all these laser sources are expensive to build and to operate.

An alternative is to compromise by restricting the wavelength range to that accessible by distributed feedback (DFB) diode lasers, while compensating for the weaker accessible

✉ Fax: +33-476-635495, E-mail: daniel.romanini@ujf-grenoble.fr, romanini.daniel@laposte.net

absorption lines by using a high sensitivity technique. DFB diode lasers are low cost, power efficient ( $\sim 10$  mW optical power from  $< 0.5$  W electric power) and operate at room temperature. They are available at any wavelength in the range 1.48 to 1.65  $\mu\text{m}$  from telecommunication companies, and are becoming available at wavelengths up to 2.7  $\mu\text{m}$  specifically selected for trace detection by specialized companies. Finally, a non-negligible benefit of working at shorter wavelengths is the high performance of near infrared photodetectors operated at room temperature (fast response and high detectivity of In-GaAs photodiodes).

In order to pursue this strategy we recently developed a technique of cavity enhanced absorption spectroscopy which exploits optical feedback (hence OF-CEAS) coming from a high-finesse cavity back to the diode laser. This technique produces temporary laser frequency locking to longitudinal cavity resonances during a laser spectral scan, providing large and reproducible cavity transmission signals and high data acquisition rates together with a large enhancement of optical absorption by molecules inside the cavity (according to the cavity enhanced principle [13]). We have described this technique and the underlying physical basis in a recent paper [14]. We also outlined its performance which make it very appealing relative to other CEAS schemes not relying on optical feedback. We will focus here on the monitoring of ambient methane by a compact and portable OF-CEAS spectrometer. After a brief description of the instrument, we will first discuss its short and long term accuracy as resulting from a prolonged comparison with a high performance chromatography setup used at LSCE (Laboratoire des Sciences du Climat et de l'Environnement, Saclay-France) which is periodically and automatically calibrated by the use of reference gas samples. We will then present another comparison with a LSD spectrometer equipped with a multipass cell [15] developed at NASA-Ames Research Center. Finally we will discuss results and performances obtained during a series of four flights aboard the NASA DC-8 aircraft.

## 2 Experimental

A picture of the OF-CEAS setup used for the methane measurements is given in Fig. 1. Also shown is the industrial PC containing most control electronics (laser temperature controller, laser current ramp, piezo mirror controller). The aluminum case used for thermal and vibrational isolation of the optomechanical assembly includes a pressure flow controller and ribbon heaters (for a peak power of 40 W). These elements were introduced to guarantee stable measurements during the flight measurement, but were not initially present when we ran the comparison with the chromatographic system. For all other measurements reported, the cell pressure was stabilized to about 400 mbar. The membrane pumps and gas delivery system used during the flight measurements are not shown.

A single rack was sufficient to integrate two similar OF-CEAS instruments inside the NASA DC8 research airplane used for the tropospheric measurement campaign. The total weight of both instruments, including gas handling (pumps and valves) was approximately 70 kg. The other instrument, operating around 1.39  $\mu\text{m}$  was dedicated to water vapor iso-

topic measurement and was developed jointly with the University of Groningen. Results and performance of this second instrument will be published elsewhere [16]. The total power consumption of the methane detector alone (including PC, pump and heaters) was about 150 W. By using optimized electronics this value could be reduced by 2–3 times.

Comprehensive details about the experimental scheme and its working principle may be found in a recent publication [14]. Briefly, a V-shaped high finesse cavity allows optical feedback to be produced only when the laser frequency enters in resonance with one of the cavity modes. Due to the properties of optical feedback locking, it is possible to obtain selective excitation of longitudinal ( $\text{TEM}_{00}$ ) cavity modes

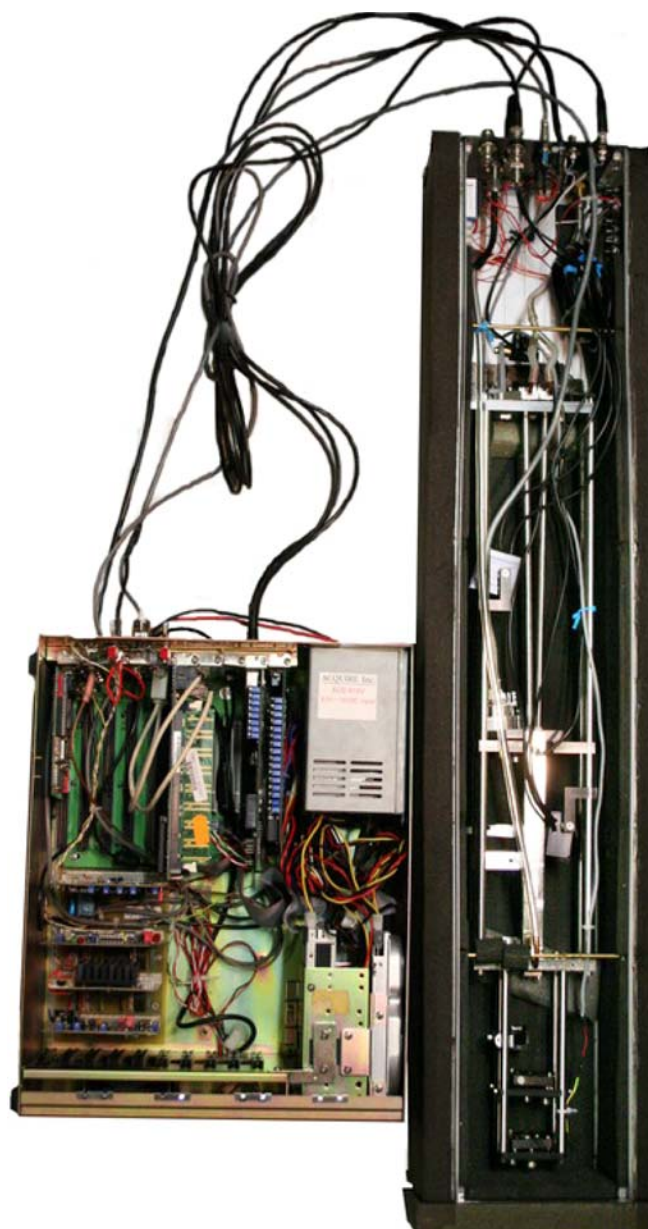


**FIGURE 1** OF-CEAS setup inside its chassis (*on the right*) as used for its integration on the DC8 airplane, together with the electronic control unit, with lids removed. Inside the industrial PC chassis there are four PC boards used for controlling the piezo-mounted mirror, and the laser current and temperature

only, yielding reproducible and low-noise cavity-enhanced spectra. An important feature is that data points in the spectra correspond to the precisely defined frequencies of these cavity modes, which are equally spaced (they are separated by the cavity free spectral range  $FSR = c/2L$ , where  $c$  is the speed of light and  $L$  is the cavity length). If the cavity is properly vibrationally isolated, the frequencies of its modes do not drift appreciably during a laser scan whose duration is short with respect to the timescale of thermal cavity length fluctuations. As the scanning time over one cavity FSR is about 0.5 ms, a 40-point absorption spectrum of an absorption line (as used for methane detection) needs a 20 ms laser current scan. The length of the cavity arms is 42.5 cm, giving  $L = 85$  cm and  $FSR = 176$  MHz. The high reflectivity mirrors, made by Research Electro-Optics (Boulder, CO), have a reflectivity of about 0.99985 in the spectral region considered, and a radius of curvature of 1 m.

The DFB diode laser is mounted inside a sealed cylindrical housing, over a Peltier element which allows its thermal stabilization to 0.001 K (short term) with 0.1 K accuracy (long term) using a home-made PID controller card. This accuracy, given a wavelength dependence on temperature of about 0.1 nm/K for DFB lasers, guarantees that the absorption line of interest will be found well centered on the typical current-driven scans we use (about  $0.4 \text{ cm}^{-1}$  wide). It is to be noted that by minimizing the size of the laser holder on the Peltier, we achieve full temperature stabilization in less than 10 s for temperature jumps of a few degrees. The laser beam is collimated (along the housing axis) via an aspheric lens with high numerical aperture. Actually, a slight focusing is provided with the focal point at the center of the cavity. Laser current ramps are supplied by a low noise home-made electronic card.

A dedicated analog circuit allows real time control (100 Hz bandpass) of the piezo-mounted mirror in order to maintain the optical phase of the feedback field to the correct value for optimal injection of cavity modes. We use a simple piezo disk which allows micrometric displacements with a low voltage control signal. The control circuit exploits the asymmetry of the cavity mode transmission patterns as an error signal [14, 17]. Indeed, the shape of the cavity modes appear strongly modified due to laser frequency locking by OF. When the OF phase is optimal, these assume a broad and rounded symmetric shape, while they become visibly asymmetric in opposite directions when the feedback phase is above or below the optimal point. Theory shows that the maximum of a modified cavity mode transmission when its shape is close to symmetric is indeed the max of the transmission function for that mode [14]. It is important to underline that small changes of the feedback phase have no consequence on the observed maximum transmission of the cavity modes even if their shape is slightly modified. Thus OF-CEAS measurements are insensitive to vibrations of small amplitude.

In our setup the diode laser can be translated along metal bars. Its position is adjusted to within a fraction of a millimeter so that the optical phase for all cavity modes injected during a laser scan is the same and the piezo-mirror position does not need to change during a laser scan [14]. Besides the optical feedback phase, another important control param-

eter is the fraction of returning radiation (feedback coupling rate). It is controlled by a variable attenuator, realized here by a polarizer rotated with respect to the diode laser polarization axis. Unlike the feedback phase, the feedback rate is adjusted only once to obtain an optimal OF locking range to cavity modes, close to the cavity FSR. The bump-shaped transmission patterns of the successive cavity modes are then sufficiently wide that they touch each other, which permits laser locking and full cavity build-up at a maximum scanning rate (about 0.5 ms/mode, as mentioned above).

In order to measure cavity input intensity and cavity transmission peaks during a laser scan, two amplified InGaAs photodiodes ( $\sim 200 \text{ k}\Omega$  transimpedance gain, 500 kHz bandpass, 1 mV r.m.s. noise) are used. A beamsplitter placed after the polarizer diverts part of the laser beam onto one of the photodiodes. The other photodiode is placed behind one of the terminal cavity mirrors. A 12-bit digitizer card (AD9812 by ADlink) installed inside an industrial PC (800 MHz pentium compact motherboard) records these two signals at a 200 kHz rate. A higher sampling rate ( $\geq 500$  kHz) is used to record, every  $N$  scans, a ringdown cavity decay (decay time about 18  $\mu\text{s}$ ). This is produced by switching off the laser current while the laser passes through resonance with a cavity mode and is optically locked to it. A timer card is used to select via software the exact instant when this should occur, to allow sampling the ringdown of a predetermined mode in the scan. This measurement sets the absolute absorption scale of the absorption spectra as described later.

The acquisition software written in C language enables efficient real time data processing, including taking the ratio of the two signals, finding the transmission maxima for all modes in each scan, and transforming the cavity transmission to absolute absorbance units (using the ringdown measurement). A Voigt lineshape fit is then used to extract the sample concentration at a rate of up to 30 Hz (using a 800 MHz pentium processor). Spectra are also streamed to a file (about 40 MB per hour of operation) to allow for successive detailed data processing.

For integration on the NASA DC8 a simple, backward facing, unheated, 9.5 mm diameter inlet enclosed in a wing-like structure was mounted on a window plate, replacing a regular window on the DC-8. A first pumping stage (N813.5 by KNF) compressed the flow to about 700 mbar. A flow controller (EL-PRESS P602C by Bronkhorst) which includes a pressure sensor and an electronic feedback loop acting on the flow valve maintained a constant pressure of 400 mbar in the sealed V-shaped high finesse measurement cell. A small second pump (N86 by KNF) generated the suction at the exhaust of the sample cell and the flow was limited by a needle valve to about 0.3 l/min STP. The compressor was only necessary because the aircraft flew sometimes at pressures below the set point in the sample cell.

Adhesive ribbon heaters (by Minco) were applied to the inside walls of the aluminum box where the optomechanical setup was installed. A small controller (also by Minco) was used to stabilize the temperature of the whole system to about 29 °C. This high setpoint was needed as the DC-8 cabin temperature before take-off could creep up above 30 °C, while during the flight it would drop down to about 15 °C. Foam lining inside and outside the box was used for thermal

and vibrational isolation. Two main reasons dictate a fixed and stable temperature operation. Firstly, our setup becomes misaligned for temperature changes of more than  $\pm 5^\circ\text{C}$  with respect to the temperature at which alignment is optimized. It should be noted that no engineering effort was made to provide a mechanical stability for wide temperature changes. Secondly, absorption line intensities depend on temperature via the Boltzmann population factor of the lower molecular level in the optical transition being probed.

### 3 Results and discussion

#### 3.1 Data analysis: From raw signals to absorption spectra

Quantitative cavity-enhanced absorption spectra may be deduced from the peak transmission values of cavity resonances obtained as the ratio of the cavity output signal over a reference laser power signal. In principle one can invert the Airy formula for the cavity transmission  $H_{\max}$  taken at the peak of a mode  $m$  [14], with respect to the absorption coefficient  $\alpha_m = \alpha(\omega_m)$ . This is possible in OF-CEAS since a full cavity buildup occurs during frequency locking by optical feedback, which at the same time also induces a laser linewidth narrowing to below the cavity mode width. We are then in a condition where the cavity is injected by a perfectly monochromatic field slowly passing through the resonance, as previously described in detail [14]. Apart from the feedback phase which must be actively controlled, and the feedback intensity which must be adjusted to a convenient level, another important requirement is that the laser tuning speed should be sufficiently slow. In these conditions, the measured values for the transmission maxima of the cavity modes will be the same as one would obtain using an ideal monochromatic light source. In our experience, and according to the theory of optical feedback, this behaviour will hold even at the limit of very high cavity finesse.

In practice, the measured value  $H_{\max}$  for a mode in the scan gives the peak transmission to within a scaling factor  $k$ . This is mainly due to the fact that the reference photodiode collects all of the laser beam profile while only part of this profile participates in the excitation of the TEM<sub>00</sub> cavity modes producing the transmission peaks. It is rather difficult to obtain the  $k$  factor directly. In addition, inversion of the Airy formula requires accurate knowledge of cavity mirror transmission and reflection coefficients. While the transmission coefficient may be obtained by a direct measurement on a cavity mirror, the reflectivity demands a ringdown measurement in the absence of intracavity gas absorption (the best solution being evacuating the cavity). In addition, both these coefficients are not constant across the mirror surface and may be subject to drift in time if the sample gas is not properly filtered.

Somewhat surprisingly, a detailed analysis reveals that in order to obtain a calibrated linear absorption spectrum we only need a single ringdown measurement, with the sample inside the cell. This is obtained by interrupting the laser while it passes through resonance with a selected cavity mode, whose position in time is deduced by the analysis of cavity transmission recorded during the previous scan. Such ringdown measurement is needed only occasionally as  $k$  does not drift rapidly. It is possible to show that the decay rate  $\gamma_m$  of the

ringdown for a mode  $m$  may be written as

$$\gamma_m = c\alpha_m - \frac{c}{L} \ln(\mathcal{R}\mathcal{R}_1) \simeq \frac{K}{\sqrt{H_{\max(m)}}}, \quad (1)$$

where  $L$  is the cavity length,  $\mathcal{R}$  and  $\mathcal{R}_1$  are the reflectivities for the V-cavity end and folding mirrors, and  $K$  is the unknown factor  $k$  multiplied by other system parameters. The first equality is the usual one for cavity ringdown measurements. It states that  $\gamma_m$  gives the absorption spectrum  $\alpha_m$  directly over a baseline which is almost constant (over a laser scan). The second approximate equality shows that the factor  $K$  (also constant over a laser scan) may be obtained from the values of  $\gamma_m$  and  $H_{\max}$  measured for a selected mode  $m$ . One may then calculate  $\gamma_m$  values for all other modes in the laser scan.

For typical cavity parameters (like those of our setup) this approximation gives a maximum fractional error of about  $5 \times 10^{-4}$  when sample absorption is strong enough to reduce the cavity transmission by a factor 100. This is approximately the limit when the cavity modes are no longer sufficiently well injected, and corresponds to an absorption coefficient of  $2 \times 10^{-5}/\text{cm}$ . Considering the noise floor on the spectra, the available dynamic range spans about four decades. This is confirmed by tests using high (but not very accurate) sample concentrations. Unfortunately, an accurate test of the linearity of response in this wide range is not trivial. Measurements presented below allow confirming of the excellent linear response in the low methane concentration range (0–2 ppm). A linear response range up to  $2 \times 10^{-5}/\text{cm}$  as expected from theory implies a maximum measurable methane concentration of 400 ppm for the R1 methane line ( $5 \times 10^{-8}/\text{cm/ppm}$  peak absorption). In addition, when reaching high concentration levels, the OF-CEAS instrument could be programmed to switch (in a few seconds needed for a laser temperature jump) to a weaker methane line thus extending the effective dynamic range for concentration measurements.

Injection by optical feedback leads to a cavity throughput close to the theoretical limit. In typical conditions, such as in the presented setup, more than 10% of the input power (tens of  $\mu\text{W}$  after the attenuator) is found in transmission at the mode maxima. CEAS and ringdown signals are thus obtained with excellent S/N ratios and the absorption scaling factor is reproducible to  $\sim 0.1\%$ . The detection limit is on the order of  $10^{-10}/\text{cm}$  for the absorption coefficient. As discussed below, we obtain this performance in the short time scale but we are currently limited by interference fringes in the spectra. These introduce small errors in the line intensities obtained from fits to line profiles. As fringe positions slowly drift in time, fit errors also drift and give long term variations on the measured concentration, on the order of 1% for the presented methane results. This analysis is confirmed by direct simulation of the signals.

In Fig. 2 we display simulated absorption spectra (from HITRAN 2004) of atmospheric molecules which may interfere with methane detection when using the R1 absorption line of the first CH-stretch overtone polyad. These simulations are based on Voigt profiles, with concentrations close to those for standard atmosphere, while pressure and temperature are those of our measurement cell. As is evident,

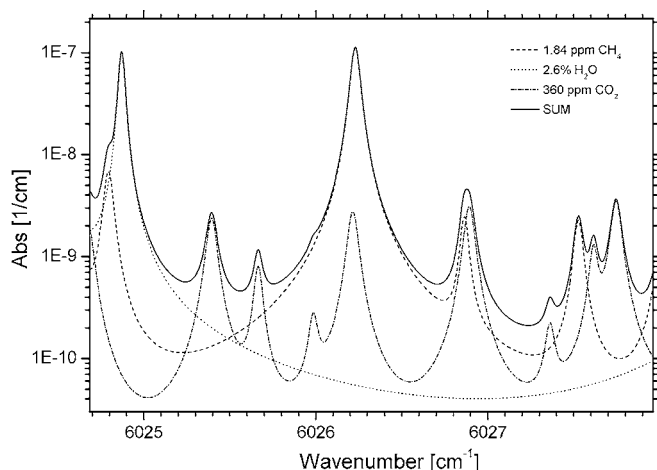


**FIGURE 2** HITRAN 2004 simulation of a small spectral region around the absorption line used here for methane monitoring. Pressure and temperature for the simulation are the same as in the measurement cell (386 mbar, 300 K). Standard concentrations are used for the atmospheric species contributing to absorption in this spectral range

there is some interference from a weak  $\text{CO}_2$  line which, for the given concentrations, has about 2% of the methane line intensity. For a change of 10% on the ambient  $\text{CO}_2$  concentration (larger than can normally be expected for this gas, except in a close human environment), an apparent change of methane concentration of 0.2%, or 4 ppb, would be induced, which is still small with respect to the  $\sim 1\%$  fluctuations for the reported ambient methane measurements. However, this choice of spectral region is clearly not satisfactory as, in addition, the R1 line is 4.5 times weaker at room temperature with respect to the R3 line (really, a multiplet) at 1653.3 nm. The R3 line would be a much better choice as it also appears to be one of the few strong methane lines in this band to be free of spectral interferences by common atmospheric species. Using the R1 line was a compromise dictated by the difficulty of finding a DFB diode laser for methane detection at the time when we started this project.

Figure 3 displays a typical spectrum (averaged over five laser scans or  $\sim 0.2$  s) obtained during the airborne measurements discussed further below, superposed with the HITRAN simulation made for the correct temperature, pressure, and concentration sample conditions. The line peak intensity is about  $10^{-7}/\text{cm}$  and the noise level (1 standard deviation) is  $\sim 2 \times 10^{-9}/\text{cm}$  on this example. Spectra taken in the laboratory in optimized conditions are at least half as noisy. The baseline value (subtracted for the sake of comparison with the simulated spectrum) corresponds to a baseline ringdown of about  $18 \mu\text{s}$ . As the cavity length is 50 cm, this implies a mirror reflectivity of 99.991%. After a Voigt fit to the line profile including a cubic polynomial to adjust for small baseline defects, the fluctuations of the derived methane concentration is at the level of a few ppbs for 1 s measurement time (averaging the results from fits of six spectra).

The spacing of data points in these OF-CEAS spectra is perfectly regular and amounts to about 300 MHz (twice the cavity FSR) since we used a setup configuration which allows selective injection of every other longitudinal cavity mode, as previously described [14]. This data point separation is suffi-

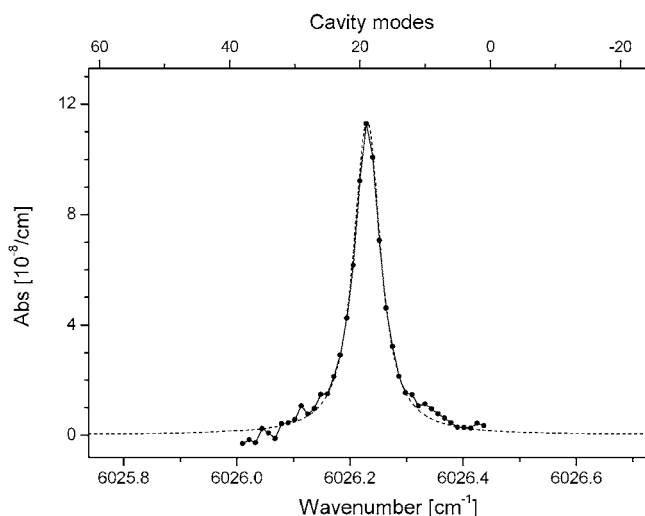


**FIGURE 3** Typical spectrum (data points linked by *continuous line*) recorded during flight measurements (horizontal scale is on the *top*). A constant bias ( $1.84 \times 10^{-6}/\text{cm}$ ) was subtracted to allow its superposition with the HITRAN 2004 simulation (*broken line*, referred to the *bottom scale*). This was calculated for a concentration of 1.84 ppm matching the intensity of the observed absorption line (same as used for the simulation in Fig. 2)

cient to trace out the profile of methane absorption lines down to pressures of about 200 mbar and allows accurate lineshape fitting using a Voigt profile with fixed Doppler width.

### 3.2 Comparison with a chromatography setup

We report here a direct comparison of methane concentration in ambient air recorded with our OF-CEAS instrument and in parallel with an automated Gas Chromatographic (GC) system (HP-6890) at LSCE. This second system is used for routine atmospheric trace measurements in flask samples collected at surface sites and for vertical profiles from airborne sampling as part of the ORE-RAMCES French monitoring network as well as for semicontinuous measurements of  $\text{CO}_2$ ,  $\text{CH}_4$ ,  $\text{N}_2\text{O}$ ,  $\text{SF}_6$  and  $\text{CO}$  [18]. The GC is equipped with two flame ionization detectors (FID) and a nickel catalyst to determine  $\text{CH}_4$ ,  $\text{CO}_2$  and  $\text{CO}$ , and an electron capture detector (ECD) for  $\text{N}_2\text{O}$  and  $\text{SF}_6$  analyse. One analysis consists of flushing the sample loops, followed by pressure and temperature equilibration, injection to the columns and analysis of the peaks. Samples are analyzed and injected every 5 min. The routine measurements sequence takes half hour including two standard gas injection and four sample analyse. The half-hourly calibration procedure of two standards allows correcting for drifts in the detector response as well as for changes of pressure and temperature which influence the amount of sample injected. This procedure uses accurately known gas mixtures from high pressure tanks, calibrated by NOAA/CMDL [19]. As a long term reproducibility and quality check, a so called “target gas” is analyzed every two hours. During the last two years the  $\text{CH}_4$  standard deviation of this target gas was better than 2 ppb.

As a first test, during 1.5 h we flushed air from a high pressure calibrated tank through the OF-CEAS instrument in order to directly assess the stability of the concentration reading and perform an accurate calibration. This allowed de-



termining of a correction to the absorption line strength of the methane line being monitored. The initial value we used was from HITRAN, whose accuracy on line intensities is typically about 10%. This yielded an average concentration for these data of 1707 ppb, with a standard deviation of 8 ppb. The LSCE GC analysis of this sample range between 1901 and 1905 ppb over an extended period (12/7/2003–29/8/2003), which gives a correction factor of 1.115 which is applied to all data measured during the following comparison test.

For a direct comparison, a continuous flow of air from outside the LSCE building was provided by a membrane pump and directed to the input of the GC system. Part of this flow was sent to the OF-CEAS instrument through a needle valve adjusted to achieve a flux of about 0.15 l/min STP, giving a flush time for the cavity volume of about 7 s. The estimated sample propagation delay along the tube going from the pump to the OF-CEAS instrument was 60 s maximum. At the time of these tests, we did not use a pressure controller and a vacuum pump to allow working at a fixed and reduced cell pressure as during the airborne tests. The cell outlet was just open to ambient and, given the small flow rate, the internal cell pressure was in equilibrium with the atmosphere.

The OF-CEAS instrument was left running continuously and unattended from the 6th to the 17th of November 2003, and the same was done for the chromatograph, with the exception of periods when flask samples had to be analyzed or maintenance was needed. OF-CEAS data were stored on a hard disk together with diagnostic parameters concerning the methane line fit and the cavity ringdown time measurement. The computers controlling the OF-CEAS and the LSCE systems were synchronized, so that the time-stamps of saved data could be directly compared.

In Fig. 4 a detailed view of the concentration as a function of time for the two instruments is given. Evident features are the delay of chromatographic data (about 15 min) and its reduced excursion during large and fast concentration variations. This is due to the use of a one liter cold trap placed before the chromatograph to freeze out the water vapor in the sample. The volume of this cold trap also integrates the am-

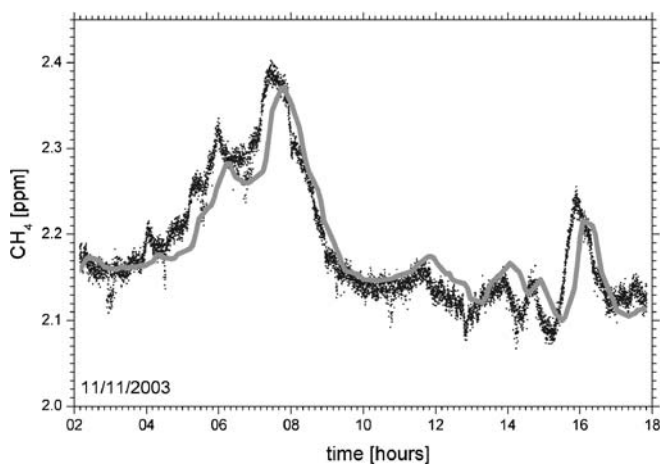


**FIGURE 4** Methane concentration time series from the OF-CEAS instrument at LSP (*dots*) and chromatographer at LSCE (*thick gray line*) for ambient methane, obtained during a 14 hours period on November 11, 2003

bient air flow over about 15 min, allowing smoothing out of the signal of the semicontinuous injections (1–8 injections per hour).

In order to allow for a closer comparison over the whole test period, we applied a 20-min binning to the OF-CEAS by averaging inside 20 min intervals to give one data point per bin (Fig. 5). We tried to vary the bin size, and 20 min allowed the best agreement with the chromatographic data, in particular its reduced peak-to-peak excursions. Finally, the chromatograph trace was time-shifted in order to eliminate its 15 min time delay. It is reassuring that the best bin size is close to this delay, which confirms that both effects are due to the cold trap. The resulting traces for the whole period are plotted in Fig. 5 together with their difference. The OF-CEAS values wander above and below the calibrated chromatographic trace over time scales of about 1 h, with max deviations typically below  $\pm 20$  ppb. The standard deviation of these residuals is 14 ppb, less than 1% of the ambient methane concentration.

To conclude, this comparison yields values in agreement to within 1% over a period of 10 days, but we are confident that our instrument would have maintained this accuracy over a much longer period, as long as temperature and pressure conditions could be kept stable. At the time of these tests our instrument was not directly thermally stabilized and the measurements were obtained at ambient pressure. However the temperature effect for the R1 methane line intensity is  $-0.33\%/K$  and the laboratory temperature was stabilized to about  $1^\circ C$ . With respect to atmospheric pressure changes (seldom exceeding 1%), the peak intensity of the collision-broadened methane line depends only on the methane relative concentration. Indeed, pressure changes at constant concentration linearly affect both the line width and its area so that the peak value remains constant. Thus, line intensity changes due to temperature or pressure variations should not contribute significantly to the observed 1% concentration fluctuations. Still, we could observe a small (below the 1% level) correlation of the deviations between the values provided by the

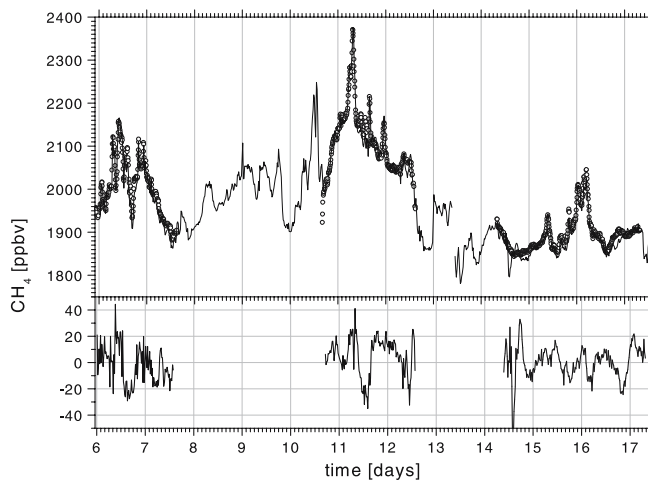


**FIGURE 5** *Top*: Ambient methane concentration time series from OF-CEAS (*line*), after time binning, and chromatography (*circles*), after correction of its response delay (see text), during several days of hands-off operation. *Bottom*: Difference between the two previous traces

two instruments with changes in the atmospheric pressure. The source of this effect might have to do with the different sampling schemes of the two instruments, and requires further investigation after which the performance of the OF-CEAS instrument will be improved.

Among other effects which could possibly affect the long-term accuracy, we should consider the loss of performance of the high reflectivity cavity mirrors. During the test period a simple mechanical filter with 3  $\mu\text{m}$  pores protected the cavity from dust in the air flow. No changes in mirror reflectivity were observed. In addition, even if over a longer period such changes cannot be excluded, these will only affect the broad band cavity losses giving the spectrum baseline (after conversion to the absorption scale as described above) and not the intensity of an absorption line laying over this baseline. It is also worthwhile to underline that most super-mirrors can be cleaned with pure solvents (acetone) without any deterioration of their dielectric coating.

In order to explain the 1% fluctuations of the OF-CEAS methane measurements around the calibrated chromatographic value, and to understand why these fluctuations are bounded (they do not grow arbitrarily large), we have to consider the presence of small fringes in the baseline of the OF-CEAS spectra. As in most spectroscopic techniques, fringing exists also in cavity enhanced spectroscopy, and may have different origins. Scattered light from the main laser beam might impinge on the reference photodiode by following an indirect path, which will produce etaloning in the normalization signal. Also, the cavity transmitted beam is from pure excitation of  $\text{TEM}_{00}$  modes, it has a clean transverse Gaussian profile, while the beam collected by the reference photodiode is a typical ‘dirty’ laser diode beam (spatial filtering is hard to implement without severely perturbing the feedback locking effect). When the laser tunes, its transverse profile might present variations which will affect the reference signal but not the cavity transmission, thus distorting the spectrum baseline. Finally, we observe small fringes due to light backscattered by the cavity output photodiode or by other surfaces along the path of the other two beams leaving the cavity. This backscattering is difficult to remove completely and the associated fringes represent the major source of fluctuations affecting the presented measurements. We ran simulations showing that drifting fringes of the observed amplitude indeed induce 1% fluctuations to the line intensity produced by a Voigt fit to the methane absorption line. In our apparatus fringes move slowly with time as the temperature drifts and the cavity modes change their position over the recorded spectrum. Since the amplitude of these fringes is not observed to increase in time, and has no reasons to do so, the induced fluctuations on concentration measurements will remain inside a fixed error range of about 1% even for time periods longer than in our test comparison.

### 3.3 Comparison with a mid-IR laser multipass spectrometer

A comparison over a few hours was performed between the OF-CEAS instrument and the mid-infrared diode laser spectrometer Argus [15] developed at NASA–Ames Research Center. This instrument includes two lead-salt diode lasers mounted inside a liquid nitrogen cooled dewar together

with four infrared detectors, plus two reference cells and a multipass sample cell. Wavelength modulation with second derivative detection is used, together with lineshape fits to retrieve the line intensities and thus the concentrations of tropospheric and stratospheric methane and other species. The two instruments were installed in parallel on a flow line from a computer-controlled mixing system generating 100%, 75%, 50%, 25%, and 0% mixtures of a calibrated standard (NOAA Climate Monitoring and Diagnostics Laboratory assigned 1752.9 ppb methane) with “zero” air (containing no  $\text{CO}_2$ , which would cause a small bias in the OF-CEAS methane levels). OF-CEAS results from fits were averaged over 2.5 s in order to achieve the same S/N ratio as Argus (3 ppb standard deviation of the noise level), whose response time was slightly faster than 2 s (multipass cell volume was 0.3 l and flow rate about 1 l/min at STP). We observe deviations above and below the Argus values on the order of  $\pm 20$  ppb consistently with previous results from the comparison with a chromatographic setup.

In Fig. 6 we show the methane concentration traces for the two instruments. The main discrepancy is a positive bias (relative to OF-CEAS) on the Argus signal at low concentrations and for the zero air sample. This corresponds to a visible second derivative signal on the Argus spectrum, while the OF-CEAS spectrum of the same sample appears flat (apart from a broad curvature and slope). Unfortunately, we cannot determine the origin of the discrepancy at this time. With respect to the OF-CEAS instrument, we can still underline the good level of agreement with Argus, which is again to within  $\pm 20$  ppb (or 1%) on a close par to atmospheric methane levels.

We may consider the linearity of the OF-CEAS instrument with respect to the concentrations generated by the mixing system (assuming zero air to have 0 ppb methane). For this, we average all recorded methane concentration values belonging to the same mixing ratio, and do a linear fit of the resulting five values against the mixing ratio. We find a perfect fit (correlation 0.99995,  $R^2 = 0.99989$ ) to within the standard deviation of each data point (0.57 ppb) in the range of 0 to 1.8 ppm.

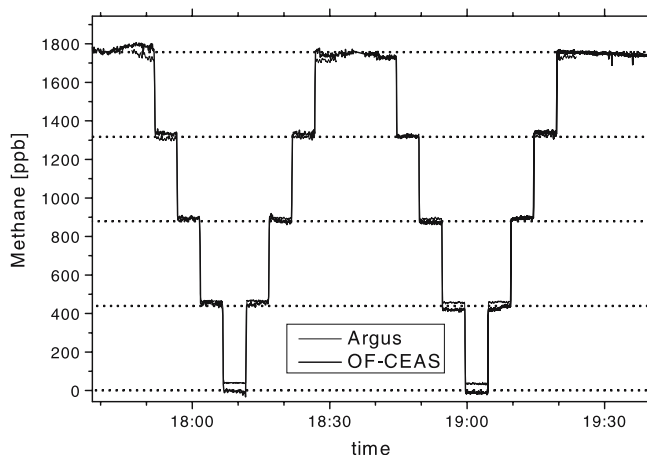
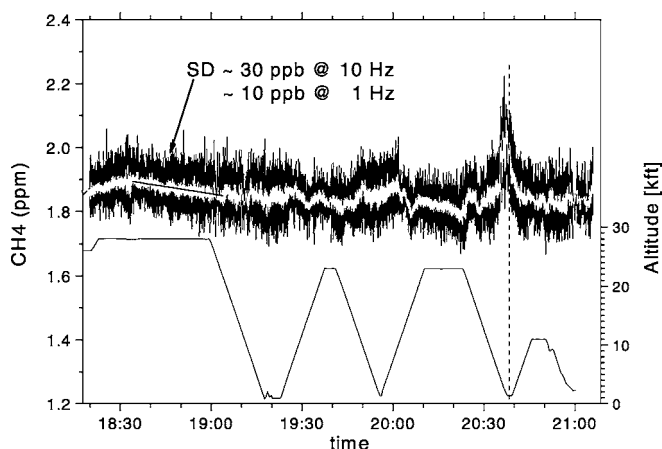


FIGURE 6 Methane concentration time series from OF-CEAS and Argus, obtained with controlled mixtures of zero-air with a methane standard of 1752.9 ppb. The horizontal dotted lines help to demonstrate the reproducibility for the same mixed sample



**FIGURE 7** Concentration of  $\text{CH}_4$  during 2.5 h of flight at various altitudes. The white trace is the 1 s averaged signal, for which the reduced noise level of 10 ppb is obtained on the short time scale by fitting a straight line to a flat interval in the trace, as shown

### 3.4 Tropospheric measurement aboard the NASA DC-8 aircraft

In Fig. 7 we show the  $\text{CH}_4$  concentration obtained during the NASA DC-8 flight of May, 12, 2004, together with the altitude profile. 1 s averaging is found to yield about 10 ppb r.m.s. noise level, while 10 Hz data shows about 30 ppb noise level, assuming this is not limited by actual atmospheric variations. This noise level is about a factor of two higher than in the laboratory and is likely due to the effect of airplane vibrations. The airplane took off from NASA Dryden and the data shown here was taken going north from San Simeon, CA along the California coast. At around 19:17 the aircraft flew 300 m above ground over the Pacific ocean near Mendocino, California. At about 19:52 another dive to 300 m above ground showed a slight increase of  $\text{CH}_4$  below altitudes of 3000 m. At 20:40 UTC there is a 10% increase in methane level in coincidence with a descent to 300 m above ground near Fresno, CA (latitude:  $36^\circ 02.1$ , longitude:  $+119^\circ 07.9$ ) which demonstrates the sensitivity of the instrument to the presence of anthropogenic sources, cattle farming in the Central Valley in this case.

## 4 Conclusions and perspectives

The OF-CEAS technique requires only a few optical components and is well adapted to the realization of compact, robust, low power, and affordable instruments for trace gas measurement. We reported here on three tests of its performance. Two of these demonstrate the ability to produce precise concentration values with high sensitivity and short response time, without need for calibration. A third test illustrates the ability to obtain field measurements in particularly harsh conditions, aboard an airplane.

As we mentioned in the experimental section, our OF-CEAS setup includes a PZT-mounted mirror which is continuously adjusted by an electronic servo-loop to maintain the phase of the optical feedback close to the right value. This adjustment occurs on the sub-wavelength level, and the position of the mirror is critical to about 100 nm. However, even with a locking band-pass of only about 100 Hz, the stiff de-

sign of the setup and its suspension inside a foam-padded box insured sufficiently stable operation even in the presence of vibrations and loud cabin noise during normal flight conditions. Only during take-off, rapid turns, and substantial atmospheric turbulence, were the measurements were disturbed by sudden shocks and rolls. In order to improve the situation, we recently changed the optomechanical layout in favor of a substantially more solid (and heavier) design. This new optical layout is currently being tested on high altitude aircrafts.

In the development of high sensitivity techniques much effort is dedicated to improve the signal to noise ratio on the vertical scale, but when it comes to spectroscopic methods, attention should be also paid to the precision on the horizontal frequency scale. This is particularly true when accurate quantitative measurements are needed, since spectral lineshape fitting is a robust method to extract accurate concentration levels. Usually, fringes from a Fabry-Pérot etalon are used as markers to linearize the frequency scan of the laser source, adding to the complexity of the optical layout. In OF-CEAS, the linearity of the frequency scale is guaranteed as the spectral data points sit on the uniform frequency comb of the  $\text{TEM}_{00}$  modes of the high finesse cavity itself.

Another strong feature of OF-CEAS is the fast acquisition rate, which can be pushed to 50 Hz for one absorption line, allowing for real time monitoring of one species with an absorption noise level as low as  $10^{-9}$  /cm. Fast spectral acquisition also guarantees that the cavity modes do not drift during the measurement. A practical limitation when using a closed cell is the sample exchange time. About 1 s response time was achieved here by using rather small sample flow rates around 0.3 l/min STP. Indeed, a definite advantage when using a high finesse cavity compared to a standard multipass cell is the much smaller sample volume. In our setup this is about  $18 \text{ cm}^3$ , and could be further reduced in the future (down to  $10 \text{ cm}^3$ ). Together with a careful hydrodynamical cell design, we expect that the sample flow time can be greatly reduced, before the onset of a turbulent regime leading to refraction index fluctuations perturbing the measurements.

Already during recent laboratory tests with the same instrument, we pushed on the flow rate and were able to observe methane concentration settling times (at the  $1/e$  level) as short as 0.3 s, limited by the flow system available. We thus believe that we are close to achieving the 10 Hz sample exchange rate which is needed for eddy correlation measurements of trace fluxes. At this sampling rate, the methane concentration is still obtained at a 1% noise level. In addition, using a recently acquired telecom DFB diode laser operating on a  $4\times$  stronger methane line (the R3 multiplet) we expect a proportional gain in sensitivity. Using better mirror coatings is also possible, as the feedback-locking scheme will work well with higher finesse cavities. However, the mirrors used here are close to the best one can get at this wavelength.

A problem which will be worth more effort to resolve, is reducing fringes in the spectrum baseline, which presently affect the detection limit and the long term accuracy. The fact that the observed deviations around the 'true' chromatographic value are due to spectral fringes explains why these deviations do not grow arbitrarily large in time but rather fluctuate inside a bounded interval. The time scale for these fluctuations depends on the thermal drift of the instrument



and corresponds to the time needed for the fringe pattern to move by one fringe interval. One important consequence is that we may be confident about the stability of the measurement over arbitrarily long periods if proper dust filtering is used. In particular, it should be noted that the mild mirror contamination does rise the spectrum baseline thus gradually reducing the dynamic range available and increasing the noise level, but it does not have any effect upon the intensity of the absorption line being measured (due to the automatic rescaling of the CEAS spectrum by absolute ringdown measurements).

A level of 1 ppb with 1 s averaging is the actual noise level for ambient methane concentration on the short-term (during a few minutes of operation). We believe we should be able to extend this figure to the long term, either after suppressing interference fringes or by “brute force” using the stronger R3 transition as mentioned above. It should be stressed that it is a different problem being able to track 1 ppb changes for a 2 ppm concentration level, which requires having a signal stable to 0.05%, and being able to detect ppb concentration levels.

With respect to the linearity, for the atmospherically relevant range of methane concentrations (0–2 ppm) we found that averaged values obtained for concentration levels generated by a gas mixing system at NASA (Fig. 6) give a perfectly linear correlation with no deviations observed inside the averaging standard deviation of 0.6 ppb. Linearity over the larger accessible dynamic range (up to 400 ppm for methane) remains to be accurately confirmed. From the physical model underlying the technique we do expect a linear response, and preliminary measurements of the OF-CEAS setup at 1.603  $\mu\text{m}$  using calibrated CO<sub>2</sub> samples indicate a linear response over three decades, but at a 2% level as limited by the accuracy of the samples.

**ACKNOWLEDGEMENTS** Financial support by the Bureau of Industrial Relations of the University J. Fourier of Grenoble is gratefully acknowledged. The DC-8 test flights were supported by NASA Ames Research Center Director’s Discretionary fund. We also thank M. Prevedelli at the Uni-

versity of Bologna for his expert advice on several issues, and D. Filippi, H. Brad for their technical support at LSCE.

## REFERENCES

- 1 J.T. Houghton, Y. Ding, D.J. Griggs, M. Noguer, P.J. van der Linden, D. Xiaosu (Eds.), *Climate Change 2001: The Scientific Basis* (University Press, Cambridge, 2001)
- 2 D.M. Cunnold, L.P. Steele, P.J. Fraser, P.G. Simmonds, R.G. Prinn, R.F. Weiss, L.W. Porter, S. O’Doherty, R.L. Langenfelds, P.B. Krummel, H.J. Wang, L. Emmons, X.X. Tie, E.J. Dlugokencky, *J. Geophys. Res.* **107**, 4225 (2005)
- 3 E.J. Dlugokencky, S. Houweling, L. Bruhwiler, K.A. Masarie, P.M. Lang, J.B. Miller, P.P. Tans, *Geophys. Res. Lett.* **30**, 1992 (2003)
- 4 M. Prather, D. Ehhalt, F. Dentener, R.G. Derwent, E.J. Dlugokencky, E. Holland, I. Isaksen, J. Katima, V. Kirchhoff, P. Matson, P.M. Midgley, H.J. Wang, *Climate Change 2001: The Scientific Basis* (University Press, Cambridge, 2001) p. 239
- 5 F. Dentener, W. Peters, M. Krol, M. van Weele, P. Bergamaschi, J. Lelieveld, *J. Geophys. Res. Atmos.* **108**, 4442 (2003)
- 6 P. Bergamaschi, M. Krol, F. Dentener, A. Vermeulen, F. Meinhardt, R. Graul, M. Ramonet, W. Peters, E.J. Dlugokencky, *Atmos. Chem. Phys.* **5**, 2431 (2005)
- 7 T. Warneke, R. de Beek, M. Buchwitz, J. Notholt, A. Schulz, V. Velasco, O. Schrems, *Atmos. Chem. Phys.* **5**, 2029 (2005)
- 8 M. Buchwitz, R. de Beek, S. Noël, J.P. Burrows, H. Bovensmann, H. Bremer, P. Bergamaschi, S. Körner, M. Heimann, *Atmos. Chem. Phys. Discuss.* **5**, 1943 (2005)
- 9 A.A. Kosterev, F.K. Tittel, *IEEE J. Quantum Electron.* **QE-38**, 582 (2002)
- 10 D. Weidmann, F.K. Tittel, T. Aellen, M. Beck, D. Hofstetter, J. Faist, S. Blaser, *Appl. Phys. B* **79**, 907 (2004)
- 11 P. Maddaloni, G. Gagliardi, P. Malarà, P. de Natale, *Appl. Phys. B* **80**, 141 (2005)
- 12 M.H. Dunn, M. Ebrahimzadeh, *Science* **286**, 1513 (1999)
- 13 A. Kastler, *Appl. Opt.* **1**, 17 (1962)
- 14 J. Morville, S. Kassi, M. Chenevier, D. Romanini, *Appl. Phys. B* **80**, 1027 (2005)
- 15 M. Lowenstein, H. Jost, J. Grose, J. Eilers, D. Lynch, S. Jensen, J. Marmie, *Spectrochim. Acta. A* **58**, 2329 (2002)
- 16 E.R.T. Kerstel, R.Q. Iannone, M. Chenevier, S. Kassi, H.-J. Jost, D. Romanini, unpublished
- 17 S.-I. Ohshima, H. Schnatz, *J. Appl. Phys.* **71**, 3114 (1992)
- 18 L. Pépin, M. Schmidt, M. Ramonet, D. Worthy, P. Ciais, *Notes des Activités Instrumentales*, note n. 13, p. 27, Institut Pierre Simon Laplace (Paris) (2001), [www.ipsl.jussieu.fr/documentation/NAI/Notes.htm](http://www.ipsl.jussieu.fr/documentation/NAI/Notes.htm)
- 19 E.J. Dlugokencky, L.P. Steele, P.M. Lang, K.A. Masarie, *J. Geophys. Res.* **99**, 17021 (1994)